

This document is the post-print Manuscript version of a Published Work that appeared in final form in CHEMICAL RESEARCH IN TOXICOLOGY, copyright © 2018 American Chemical Society. To access the final edited and published work see <http://dx.doi.org/10.1021/acs.chemrestox.8b00216>

Design, synthesis and biological activity of hydrogen peroxide responsive arylboronate melatonin hybrids

Annalida Bedini,^{†Δ} Alessandra Fraternali,^{‡Δ} Rita Crinelli,[‡] Michele Mari,[†] Silvia Bartolucci,[†] Laura Chiarantini,^{‡*} Gilberto Spadoni^{†*}

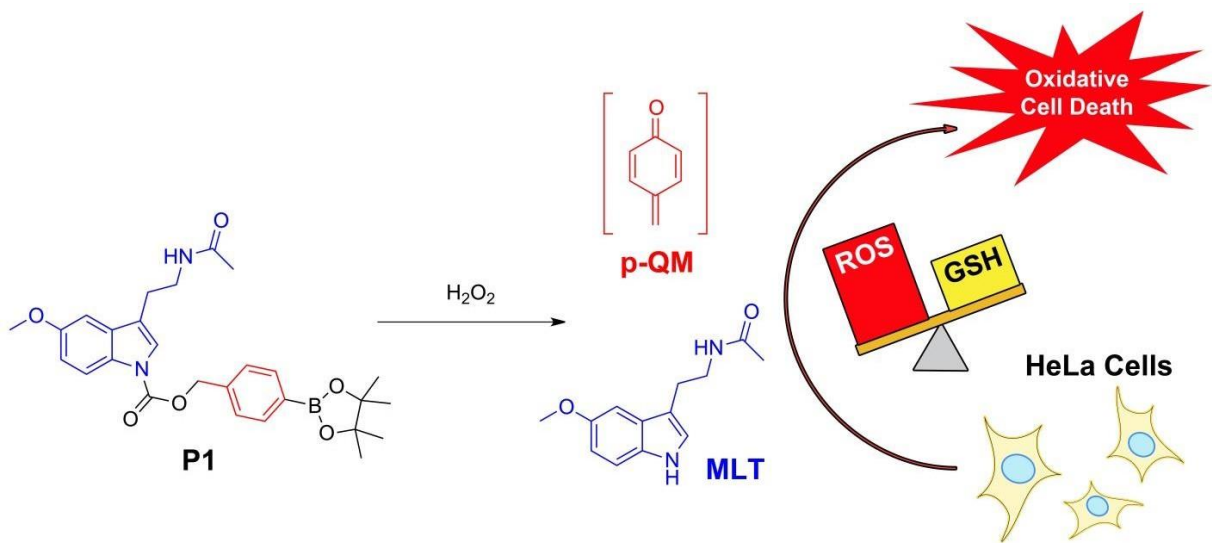
^ΔThese authors equally contributed to this work

* Corresponding authors

[†]Department of Biomolecular Sciences, University of Urbino Carlo Bo, Piazza Rinascimento 6, I-61029 Urbino, Italy.

[‡]Department of Biomolecular Sciences, University of Urbino Carlo Bo, Via Saffi 2, I-61029 Urbino, Italy.

Table of Contents graphic



ABSTRACT

Stimulus-responsive cleavage reactions have found broad use to direct drug release at a particular target disease area. Increased levels of reactive oxygen species (ROS) have been associated with the development and progression of cancer and several other disease states, motivating the development of drug conjugates that can undergo a chemoselective ROS-triggered release. Melatonin (MLT) and the reactive electrophile *p*-benzoquinone methide (*p*-QM) have evidenced either cytoprotective and cytotoxic effects in biological systems, depending on the dose, cellular targets, and time of exposure. In this study we report the synthesis and biological activity of two MLT derivatives linked to ROS-responsive arylboronate triggers (**P1** and **P2**), which can be activated by endogenously generated hydrogen peroxide (H₂O₂) to release MLT, or 5-methoxytryptamine (5-MeOT), and *p*-QM-intermediates. Their H₂O₂-induced activation mechanism was studied by HPLC-DAD-MS. **P1**, which rapidly releases MLT and *p*-QM, was able to strongly induce the Nrf2 antioxidant signaling pathway, but was ineffective to provide protection against H₂O₂ mediated oxidative damage. By contrast, **P1** exhibited strong toxic effects in HeLa cancer cells, without causing significant toxicity to normal NCTC-2544 cells. Similar, although more limited, effects were exerted by **P2**. In both cases, cytotoxicity was accompanied by depletion of cellular glutathione (GSH), probably as a consequence of *p*-QM release, and increased ROS levels. A role for MLT in toxicity was also observed, suggesting that the **P1** released products, MLT and *p*-QM, contributed additively to promote cell death.

INTRODUCTION

Maintenance of redox homeostasis plays a central role in health and disease prevention, and alteration of this delicate balance can lead to pathological consequences. Overproduction of hydrogen peroxide (H_2O_2) and other reactive oxygen species (ROS) in normal cells causes oxidative stress that is thought to contribute to the onset and development of neurodegenerative¹, cancer² and cardiovascular³ diseases, as well as ischemic stroke and diabetes⁴. Therefore, oxidative stress containment is paramount for cell functionality. To counteract oxidative stress, cells have developed endogenous defense mechanisms, including the activation of nuclear factor erythroid 2–related factor 2 (Nrf2),⁵ a transcription factor controlling the expression of various cytoprotective and antioxidant enzymes.⁶⁻⁸ In the last few decades, many studies have demonstrated the benefits of several natural products in counteracting oxidative stress through modulation of the Nrf2/Antioxidant Response Element (ARE) signaling pathway.⁹ Nevertheless, cancer cells, compared with normal cells, generate higher amounts of ROS, including H_2O_2 , and adapt to oxidative stress by increasing their antioxidant capacity, such as enhancing the synthesis of the antioxidant glutathione (GSH), to counteract the damaging effects of ROS.^{10,11} The higher levels of ROS in tumor cells can be exploited to enhance selectivity and therapeutic activity of antitumor agents¹², and exogenous compounds increasing oxidative stress preferentially in cancer cells can potentially be used as anticancer drugs.¹³

The tryptophan-derived hormone melatonin (MLT) is a well-known multifunctional molecule mainly secreted by the pineal gland during the night. It influences a number of functions of the central nervous system such as the synchronization of circadian rhythms, the regulation of the sleep-wake cycle, the control of mood and behavior, hormone secretion and many others.¹⁴ Peripherally, MLT is involved in the modulation of the immune system, of retinal functions, of the cardiovascular system and in glucose homeostasis.¹⁵ A beneficial role of MLT administration has also been proposed for neurodegenerative diseases, diabetes, multiple sclerosis and cancer.^{16,17} A feature that characterizes MLT is the variety of mechanisms it employs to modulate the cell physiology. Its functions primarily depend on G protein-coupled transmembrane receptors, named MT_1 and MT_2 , mainly expressed in

the central nervous system, but also detected in many peripheral tissues.¹⁸ Apart from its receptor-mediated actions, MLT is a powerful antioxidant that scavenges free radicals¹⁹ or activates the Nrf2/ARE signal pathway, thereby promoting anti-oxidant enzyme expression.²⁰⁻²²

Melatonin has also attracted attention as a natural oncostatic agent that can suppress neoplastic growth in a variety of tumors.²³ Although epidemiological studies concerning the association between body circadian melatonin levels and cancer incidence have led to controversial conclusions,²³ accumulating evidence from *in vitro* studies and animal models has supported the anticancer properties of MLT.^{24,25} Melatonin can exert its antitumor activity by induction of apoptosis and epigenetic alteration, interaction with melatonin receptors, as well as by inhibition of angiogenesis, invasion and metastasis.²⁶ Preliminary clinical studies in patients with cancer have also demonstrated that MLT can reinforce the therapeutic efficacy and/or reduce the side effects of the cancer chemotherapeutic agents.^{27,28} The anticarcinogenic action of MLT has also been related, in part, to its potent antioxidant activity, although recent evidence has indicated that MLT may exert pro-oxidant action in tumor cells.^{29,30} Thus, the effects of MLT seem to be context specific allowing normal cells to be spared while killing cancer cells.³¹

Quinones, including quinone imines and quinone methides represent a class of toxicological intermediates, which can alter redox balance within cells. These compounds can induce a variety of hazardous effects *in vivo*, but they could be also exploited for therapeutic purposes, predominantly in the field of cancer chemotherapy. Bioactivation of small molecules resulting in the production of electrophilic reactive intermediates is often considered a risk factor in drug development. However, there are several examples of biologically active compounds containing such reactive electrophiles, notably Michael acceptors such as *p*-benzoquinone methide (*p*-QM), which have demonstrated promising cancer chemopreventive and chemotherapeutic activity.^{32,33}

For example, interesting chemopreventive and antiproliferative effects in cell cultures and animal models were reported for the hydroxybenzyl-linked NO-aspirin hybrids (*p*NO-ASA), or their *p*-substituted-ASA congeners not containing an NO-donating group, as the result of bioactivation to *p*-

QM.³⁴⁻³⁶ Cytoprotection was attributed to formation of QM which covalently modifies the repressor protein Keap1, leading to activation of Nrf2 and subsequent induction of detoxifying enzymes.³⁷ Similarly, QM is able to induce toxic effects through covalent modification of a variety of other nucleophiles including DNA, causing genotoxicity, and GSH altering cell redox balance. It is now becoming generally accepted that quinones have opposing effects in biological systems which, depending on the dose, cellular targets, and time of exposure, could result in toxicity or cytoprotection.^{38,39}

In light of the pleiotropic profile of MLT and the current interest in electrophilic drugs, we have hypothesized that the combination of these compounds in one molecule could eventually result in additive cytoprotective or cytotoxic effects. Aryl boronic esters are relatively easy to synthesize, generally biocompatible, and react selectively with ROS in a B-C bond cleavage reaction to release the corresponding phenolate.⁴⁰ Thus, a strategy was employed to design melatonin derivatives linked to ROS-responsive arylboronate triggers (Figure 1), which can be activated by endogenously generated H₂O₂ to release MLT or 5-methoxytryptamine (5-MeOT), and *p*-QM intermediates. These molecules are expected to have a potential therapeutic application for oxidative stress-related diseases and/or cancer, acting as mediators of cytoprotective or cytotoxic responses.

performance liquid chromatography (HPLC), was greater than 95%. These analyses were performed on a Waters HPLC/DAD/MS system (separation module Alliance HT2795, Photo Diode Array Detector 2996, mass detector Micromass ZQ; software: MassLynx 4.1) using a Gemini 5 μ C6-Phenyl 110A column (150 x 4.60 mm, 5 μ m). Method: linear gradient from a mixture 50/50 (v/v) CH₃CN/HCOOH 0.1% in H₂O to a 90/10 mixture in 8 minutes and then from 90/10 mixture to 100% CH₃CN in 2 min; flow rate: 1 mL min⁻¹, injection volume 10 μ L, UV detection at λ = 254 nm (**P1**, R_t = 6.13 min; **P2**, R_t = 6.70 min).

4-(4,4,5,5-Tetramethyl-1,3,2-dioxaborolan-2-yl)benzyl 3-(2-acetamidoethyl)-5-methoxy-1H-indole-1-carboxylate (**P1**). *4-(4,4,5,5-Tetramethyl-1,3,2-dioxaborolan-2-yl)benzyl 1H-imidazole-1-carboxylate*⁴¹ (180 mg, 0.55 mmol) and DBU (40 μ L) were added to a solution of MLT (116 mg, 0.5 mmol) in dry CH₃CN (2.5 mL). The resulting mixture was stirred under N₂ atmosphere, at 50°C for 7 h. The solvent was evaporated under reduced pressure and the crude residue was purified by silica gel flash chromatography (EtOAc as eluent). Amorphous solid, mp 148-9 °C, 70% yield. ¹H NMR (400 MHz, CDCl₃): δ 1.34 (s, 12H), 1.93 (s, 3H), 2.85 (t, 2H, *J* = 6.5 Hz), 3.55 (m, 2H), 3.84 (s, 3H), 5.41 (s, 2H), 5.80 (brs, 1H), 6.92 (dd, 1H, *J* = 2.0 and 9.0 Hz), 6.99 (d, 1H, *J* = 2.0 Hz), 7.41 (brs, 1H), 7.46 (d, 2H, *J* = 8.0 Hz), 7.86 (d, 2H, *J* = 8.0 Hz), 8.03 (brs, 1H). ¹³C NMR (100 MHz, CDCl₃): δ 170.2, 156.2, 150.6, 138.0, 135.2, 134.9, 131.3, 127.6, 123.3, 118.6, 116.1, 113.3, 101.8, 83.9, 68.5, 55.7, 39.0, 25.1, 24.8, 23.3. ESI MS (*m/z*): 493 (M+H)⁺. HRMS (ESI): *m/z* calculated for C₂₇H₃₄N₂O₆B, [M+H]⁺ 493.2510. Found: 493.2599.

4-(4,4,5,5-Tetramethyl-1,3,2-dioxaborolan-2-yl)benzyl (2-(5-methoxy-1H-indol-3-yl)ethyl)carbamate (**P2**). 4-Nitrophenyl *4-(4,4,5,5-tetramethyl-1,3,2-dioxaborolan-2-yl)benzyl carbonate*⁴² (180 mg, 0.47 mmol) and TEA (0.28 mL) were added to a solution of 5-methoxytryptamine⁴³ (90 mg, 0.47 mmol) in dry CH₂Cl₂ (5 mL). The resulting mixture was stirred

under N₂ atmosphere, at room temperature (RT) for 16 h. The solvent was removed by distillation under reduced pressure and the crude residue was purified by silica gel flash chromatography (cyclohexane-EtOAc 7:3 as eluent) and crystallization. White solid, mp 161-2 °C (CH₂Cl₂-petroleum ether); 52% yield. ¹H NMR (400 MHz, CDCl₃): δ 1.35 (s, 12H), 2.95 (t, 2H, *J* = 6.5 Hz), 3.54 (m, 2H), 3.85 (s, 3H), 4.86 (brs, 1H), 5.12 (s, 2H), 6.87 (dd, 1H, *J* = 2.5 and 8.5 Hz), 6.99 (m, 1H), 7.03 (m, 1H), 7.26 (d, 1H, *J* = 8.5 Hz), 7.34 (d, 2H, *J* = 8.0 Hz), 7.80 (d, 2H, *J* = 8.0 Hz), 7.93 (brs, 1H). ¹³C NMR (100 MHz, CDCl₃): δ 156.3, 154.1, 139.7, 134.9, 131.5, 127.6, 127.1, 122.8, 112.6, 112.4, 111.9, 100.5, 83.8, 66.4, 55.9, 41.2, 29.7, 25.7, 24.8. ESI MS (*m/z*): 451 (M+H)⁺. HRMS (ESI): *m/z* calculated for C₂₅H₃₂N₂O₅B, [M+H]⁺ 451.2404. Found: 451.2361.

Sensitivity to H₂O₂. The ability of **P1** and **P2** to release two different end-units (*p*-QM and MLT or 5-MeOT) in the presence of H₂O₂ was evaluated by HPLC-DAD-MS. Analyses were performed at 25°C on a Waters HPLC/DAD/MS system (separation module Alliance HT2795, Photo Diode Array Detector 2996, mass detector Micromass ZQ; software: MassLynx 4.1) using a Gemini 5μ C6-Phenyl 110A column (150 x 4.60 mm, 5 μm). Hybrids **P1** and **P2** were solubilized in a 1:1 v/v CH₃CN/physiological buffer saline (PBS, 5 mM sodium phosphate buffer, 0.9% (w/v) NaCl, pH 7.5) mixture to a final concentration of 1 mg/mL and treated (or not) with 20 equivalents of 40% m/v H₂O₂ at RT. At various time points the mixture was subjected to HPLC analysis. Mobile phase: linear gradient from a 10/90 (v/v) mixture CH₃CN/HCOOH 0.1% in H₂O to a 90/10 mixture in 8 minutes and then 90/10 mixture for 2 min; flow rate: 1 mL min⁻¹, injection volume 10 μl, UV detection at λ = 278 nm.

Cell culture and treatments. Human keratinocyte (NCTC-2544) cell line was grown in Dulbecco's Modified Eagle Medium (DMEM) supplemented with 2 mM L-glutamine, 7% heat-inactivated fetal bovine serum (FBS), 100 U/mL penicillin and 10 μg/mL streptomycin. Human epithelioid cervix carcinoma (HeLa) cell line was grown in RPMI supplemented with 2 mM L-glutamine, 10% heat-

inactivated FBS, 100 U/mL penicillin and 10 µg/mL streptomycin. Cells were cultured under a humidified atmosphere containing 95% air and 5% CO₂ at 37°C. Dimethyl sulfoxide (DMSO) was used as a vehicle to enable full solubility of the tested compounds MLT, 5-MeOT, **P1** and **P2** in the stock solutions (100 mM) that were stored at -80 °C.

Cells were treated with various concentrations (ranging from 1 to 100 µM) of MLT, 5-MeOT, **P1** and **P2** and DMSO did not exceed 0.1% (v/v). Cells treated with DMSO at final concentration 0.1% (v/v) were used as control.

Cell viability assay. Cell viability was evaluated using the MTS (3-(4,5-dimethylthiazol-2-yl)-5-(3-carboxymethoxyphenyl)-2-(4-sulfophenyl)-2H-tetrazolium) tetrazolium assay (Cell Titer 96® Aqueous, Promega, Madison, WI, USA) as previously reported.⁴⁴ This assay is based on the reduction of the MTS tetrazolium compound by viable cells to generate a colored formazan dye that is soluble in cell culture media. This conversion is thought to be carried out by NAD(P)H-dependent dehydrogenase enzymes in metabolically active cells. Briefly, cells were seeded in 96-well microtiter plates at a density of 5 x 10³ and 2 x 10³ cells/well for NCTC-2544 and HeLa cells respectively and subsequently exposed to **P1**, **P2** MLT and 5-MeOT, at different concentrations (ranging from 0 to 100 µM) for 24 or 48 h. After the treatments, 20 µl of MTS were added into each well, and then incubated for 30 min at 37°C; the plates were read in a Benchmark microplate reader (BioRad, Hercules, CA, USA) at 490 nm at a reference wavelength of 630 nm.

In some experiments, HeLa cells were seeded in 24 well plates at a density of 1.2 x 10⁴ cells/well and treated with 10, 50 and 100 µM **P1** for 24 h; the number of live and dead cells was counted by trypan blue staining: 20 µl of cell suspension was mixed with 20 µl of trypan blue 0.4% solution (Sigma-Aldrich, UK) and the cells were counted using Countess II Automated Cell Counter (Thermo Fisher Scientific, USA).

Nrf2 activation. Nrf2 activation was assessed in NCTC-2544 cells pre-incubated overnight (o/n) in serum-free medium (-FBS) in the presence or absence (NT) of the tested compounds **P1**, **P2** or MLT (100 μ M, unless otherwise specified). The day after, the medium was removed and the cells were maintained in culture with FBS-supplemented medium (+FBS) for up to 7 h. At time 0, 2, 4 and 7 h cells were harvested for nuclear extraction and western immunoblotting analysis.

In some experiments the medium containing FBS was supplemented with 10 mM GSH-C4 (kindly provided by GLUOS S.r.l., Urbino) and cells were harvested after 4 h incubation.

Nrf2 activation was also assayed in HeLa cells incubated with **P1** or **P2** (100 μ M) under standard growth conditions. At time 0, 1.5, 3, 6, 8 h, cells were washed in PBS and whole cell lysates were submitted to western immunoblotting analysis.

Cell lysis and nuclear fractionation.

For nuclear protein extraction, cells were washed with PBS and lysed in hypotonic Buffer A [10 mM Hepes/KOH pH 7.9, 10 mM KCl, 0.1% (v/v) Nonidet-P40], supplemented with a cocktail of protease inhibitors (Roche). After centrifugation at 14,000 x *g* at 4°C for 10 min., the pellet was suspended in hypertonic Buffer B (20 mM Hepes/KOH pH 7.9, 25% glycerol, 0.42 M NaCl), supplemented with protease inhibitors. Nuclear proteins were recovered by centrifugation at 14,000 x *g* in the supernatant.⁴⁵ Protein concentration was determined by the method of Bradford, using bovine serum albumin as standard.

Whole lysates were obtained by directly harvesting the cells in Sodium Dodecyl Sulfate (SDS) buffer (50 mM Tris-HCl, pH 7.8, 0.25 M sucrose, 2% (w/v) SDS, 10 mM *N*-ethylmaleimide supplemented with protease inhibitors as above). Lysates were boiled for 5 min, then sonicated at 100 Watts for 20 sec. Cell debris was removed by centrifugation at 14,000 x *g* at room temperature. Protein content was determined by the Lowry assay.

Western immunoblotting analysis

Equal amounts of proteins were resolved by SDS-PAGE and gels were electroblotted onto a nitrocellulose membrane (0.2 μm pore size) (BioRad laboratories Inc.). The blots were probed with anti Nrf2 antibody (D1Z9C, Cell Signaling Technology). Anti Ying Yan 1 antibody (YY1, C-20, sc-281) (Santa Cruz Biotechnology Inc.) was used as nuclear loading control. Anti actin (A 2066, Sigma) was used to check equal protein loading for whole cell lysates. Bands were detected by horseradish peroxidase (HRP)-conjugated secondary antibody (BioRad) and the enhanced chemiluminescence detection kit WesternBright ECL (Advasta).

Flow cytometric analysis of ROS. Intracellular ROS levels were measured by flow cytometry using 2',7'-dichlorodihydrofluorescein diacetate (H2-DCF-DA, Sigma-Aldrich), which easily diffuses into cells where it is transformed by esterases to 2',7'-dichlorodihydrofluorescein (H2-DCF). This membrane-impermeable product is then oxidized to the highly fluorescent 2',7'-dichlorofluorescein (DCF) by intracellular ROS, primarily by H_2O_2 .⁴⁶ NCTC-2544 and HeLa cells were plated at a density of 8×10^4 and 2.6×10^4 cells per well in 24 well plates, respectively. The day after the medium was removed and substituted with fresh medium containing the tested compounds **P1**, **P2** or MLT at a concentration of 100 μM for 6 h. The cells were harvested by trypsin and suspended in 1 mL PBS supplemented with 3% (v/v) FBS. Then 2×10^5 cells were labeled with 10 μM H2-DCF-DA for 30 min at RT in the dark and immediately analyzed for DCF fluorescence using a FacScan flow cytometer (Becton Dickinson).

GSH determination. GSH levels in NCTC-2544 and HeLa cells treated with the tested compounds **P1**, **P2** or MLT (100 μM) o/n were determined following the previously described procedure.⁴⁷ Briefly, the cells were washed twice in PBS and immediately lysed with 100 μL of lysis buffer (0.1% Triton X-100, 0.1 M Na_2HPO_4 , 5 mM EDTA, pH 7.5). Thereafter, 15 μL of 0.1 N HCl and 140 μL of precipitating solution (100 ml containing 1.67 g of glacial metaphosphoric acid, 0.2 g of disodium EDTA, 30 g of NaCl), were added. After centrifugation at 12,000 x g for 10 min, the supernatant was

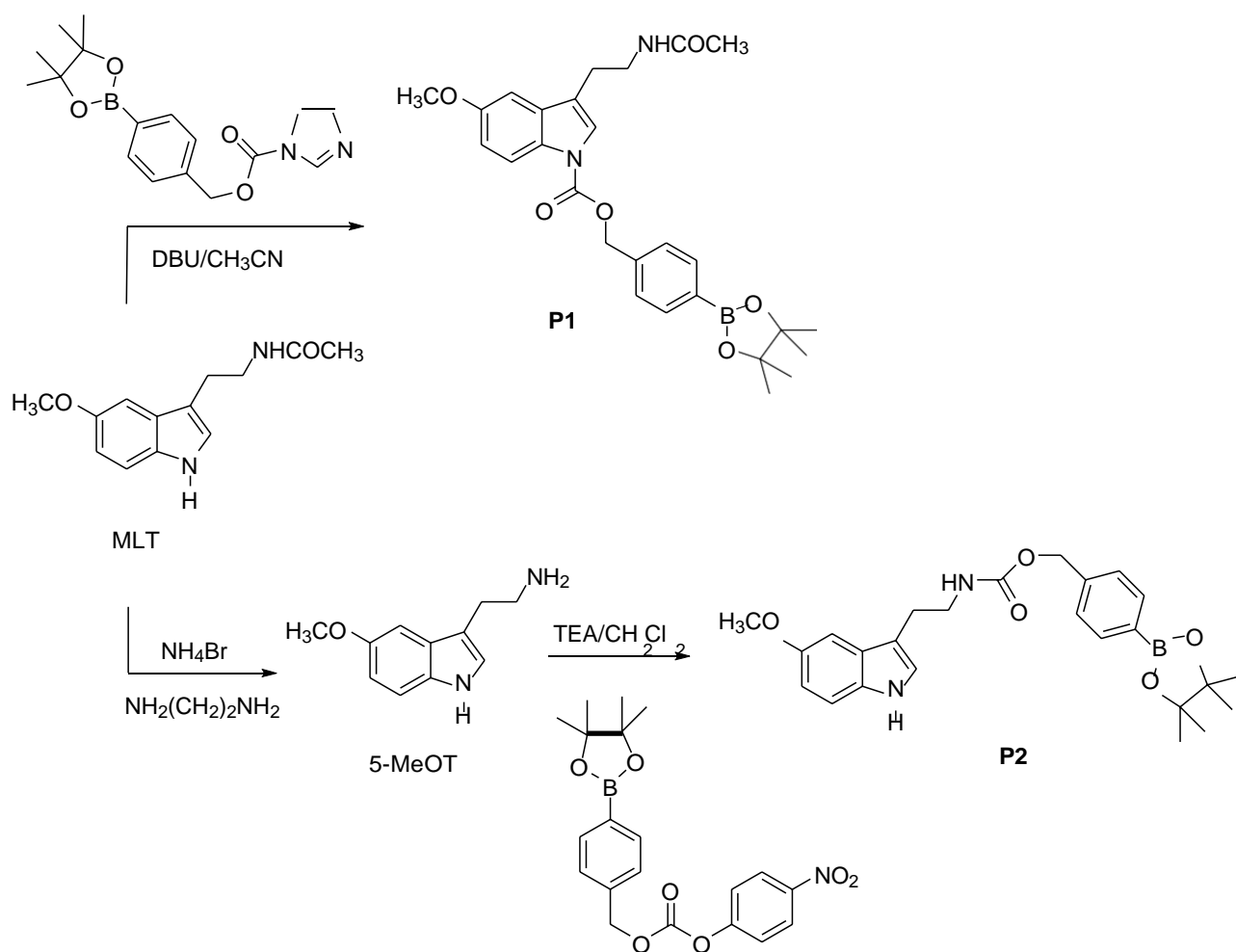
collected and 25% (v/v) 0.3 M Na₂HPO₄ and immediately after 10% (v/v) 5,5'-dithio-bis(2-nitrobenzoic acid) (DTNB) were added. The mixture was stirred for 1 min at RT, then left at RT for another 5 min, and finally used for HPLC determination of thiols.⁴⁸

Statistical analysis. Statistical analysis was performed with GraphPad InStat. Data were analyzed with the two-tail paired Student's t test for pairwise comparisons or one-way analysis of variance (ANOVA) for multiple comparisons. A *P* value of less than 0.05 was considered significant.

RESULTS and DISCUSSION

Design and synthesis of melatonin-arylboronate hybrids. Taking into account the properties of MLT and *p*-QM we synthesized two new hybrid compounds (**P1** and **P2**) by coupling MLT or 5-MeOT with a *p*-boronate benzyl moiety through a carbamate linkage (Figure 1), that would be inert under normal physiological conditions, but potentially able to release multiple active species in response to high levels of ROS. A selective oxidative hydroxylation of the arylboronate trigger unit by H₂O₂ should provide the corresponding phenol in equilibrium with phenolate (and the non toxic boric acid or its pinacolate ester), which spontaneously could decompose to *p*-QM, CO₂ and MLT or 5-MeOT (see also Scheme 2 and 3).

The designed melatonin-arylboronate **P1** was prepared by *N*¹-carbamoylation of MLT with 4-(4,4,5,5-tetramethyl-1,3,2-dioxaborolan-2-yl)benzyl 1*H*-imidazole-1-carboxylate which in turn was obtained by treating 4-(hydroxymethyl)phenylboronic acid pinacol ester with carbonyldiimidazole following a previously reported procedure⁴¹ (Scheme 1). To prepare the target hybrid compound **P2**, MLT was first converted into 5-MeOT by microwave-assisted deacetylation using a combination of ammonium bromide and ethylenediamine⁴³, and then submitted to *N*-carbamoylation by treatment with 4-nitrophenyl (4-(4,4,5,5-tetramethyl-1,3,2-dioxaborolan-2-yl)benzyl) carbonate⁴² (Scheme 1).



Scheme 1. Synthesis of pinacol arylboronate melatonin derivatives.

H₂O₂-induced transformation of hybrids P1 and P2. The *in vitro* stability of hybrids **P1** and **P2** in the absence of H₂O₂ (Figures 2 and 3) and their H₂O₂-induced (20 equiv) cleavage/activation (Figures 4 and 5) were followed by HPLC-DAD-MS. Compounds **P1** and **P2** when incubated in PBS partially converted to their corresponding acids, as highlighted by the appearance of the peak at retention time (R_t) 6.65 min ($[M+H]^+ = 411$, Figure 2) or the peak at $R_t = 6.68$ min ($[M+H]^+ = 369$, Figure 3).

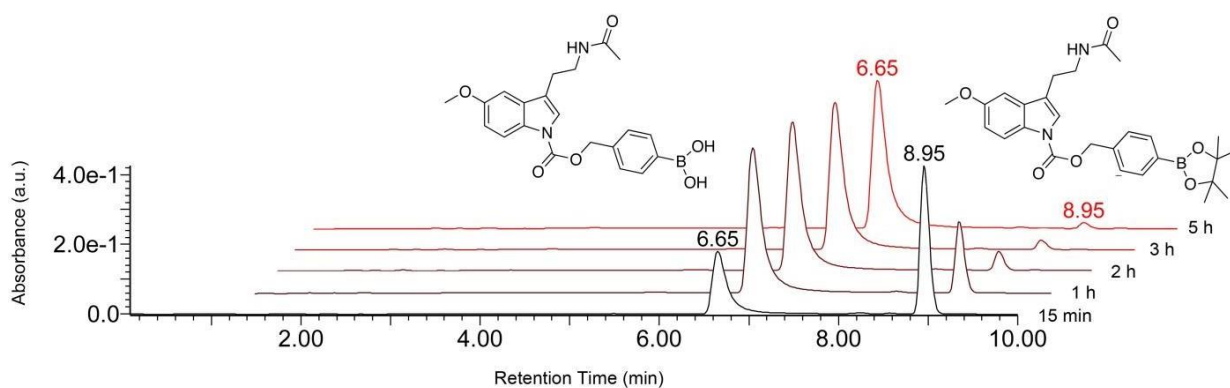


Figure 2. Stability of **P1** ($R_t = 8.95$ min) and its corresponding boronic acid ($R_t = 6.65$ min) in the absence of H_2O_2 .

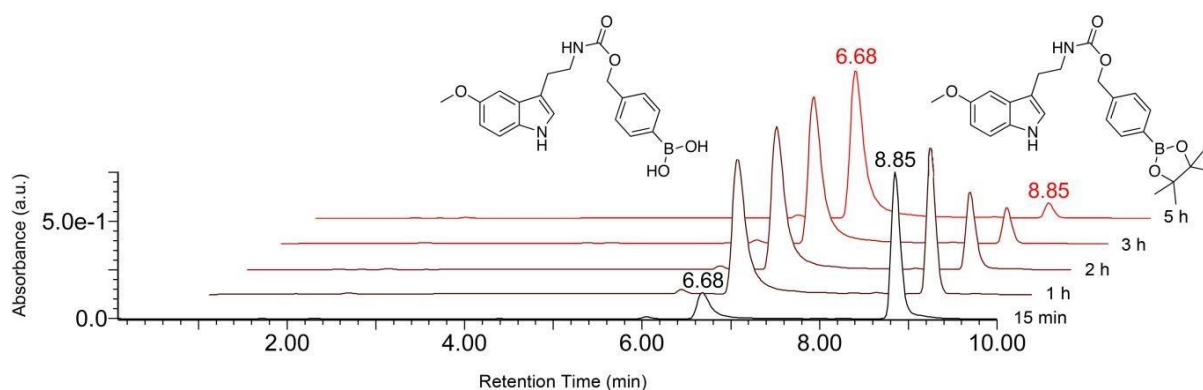


Figure 3. Stability of **P2** ($R_t = 8.85$ min) and its corresponding boronic acid ($R_t = 6.68$ min) in the absence of H_2O_2 .

Upon treatment of **P1** with H_2O_2 we observed complete disappearance of the compound, and of its corresponding boronic acid, within 5-15 min, which is in accordance with previous reports suggesting fast reactivity of arylboronic acids and their esters with H_2O_2 .⁴⁹ Formation of a new peak after 15 min corresponding to *p*-hydroxybenzyl alcohol (*p*-HBA, resulting from the scavenging of *p*-QM by water,

$R_t = 3.52$ min), and of another peak corresponding to the intermediate 1-carboxy-MLT (**B**, $R_t = 6.52$ min, $[M+H]^+ = 277$) which decomposed over a period of 7 h to generate MLT ($R_t = 5.52$ min, $[M+H]^+ = 233$), suggested the formation of the intermediate undetected phenolate **A**, which spontaneously and irreversibly undergoes a 1,6-elimination to release *p*-QM and **B** (Scheme 2).

The formation of *p*-HBA is in good agreement with previous studies reporting that *p*-QM is converted to *p*-hydroxybenzyl alcohol under aqueous conditions in the absence of nucleophiles such as GSH.³⁵ Indeed, *p*-HBA was not observed neither in positive nor in negative detection mode in the ESI mass spectra of the mixture, as already reported in similar cases.⁵⁰ However, its formation was proved in HPLC-DAD (or TLC) by an authentic sample, the peak of which matched exactly with that of the above cited *p*-HBA (Figures S1 and S2).

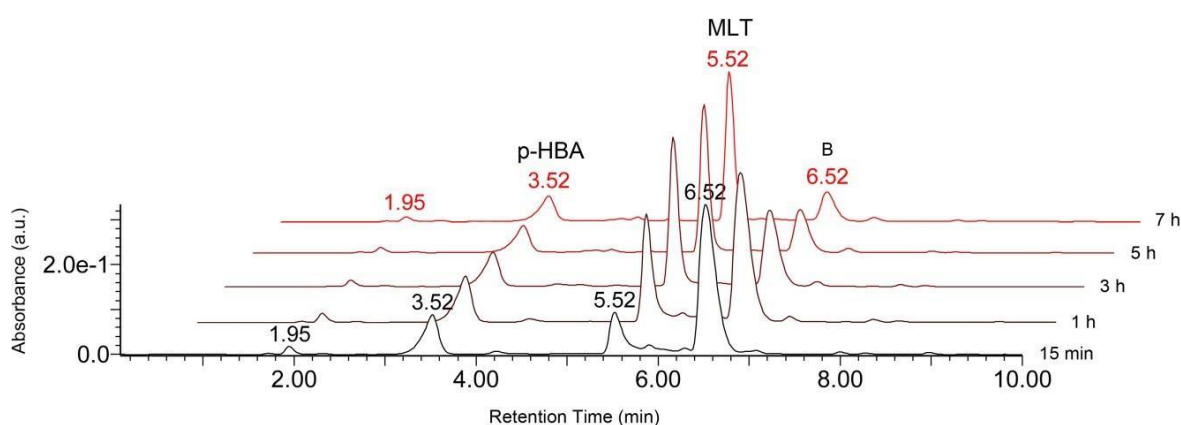
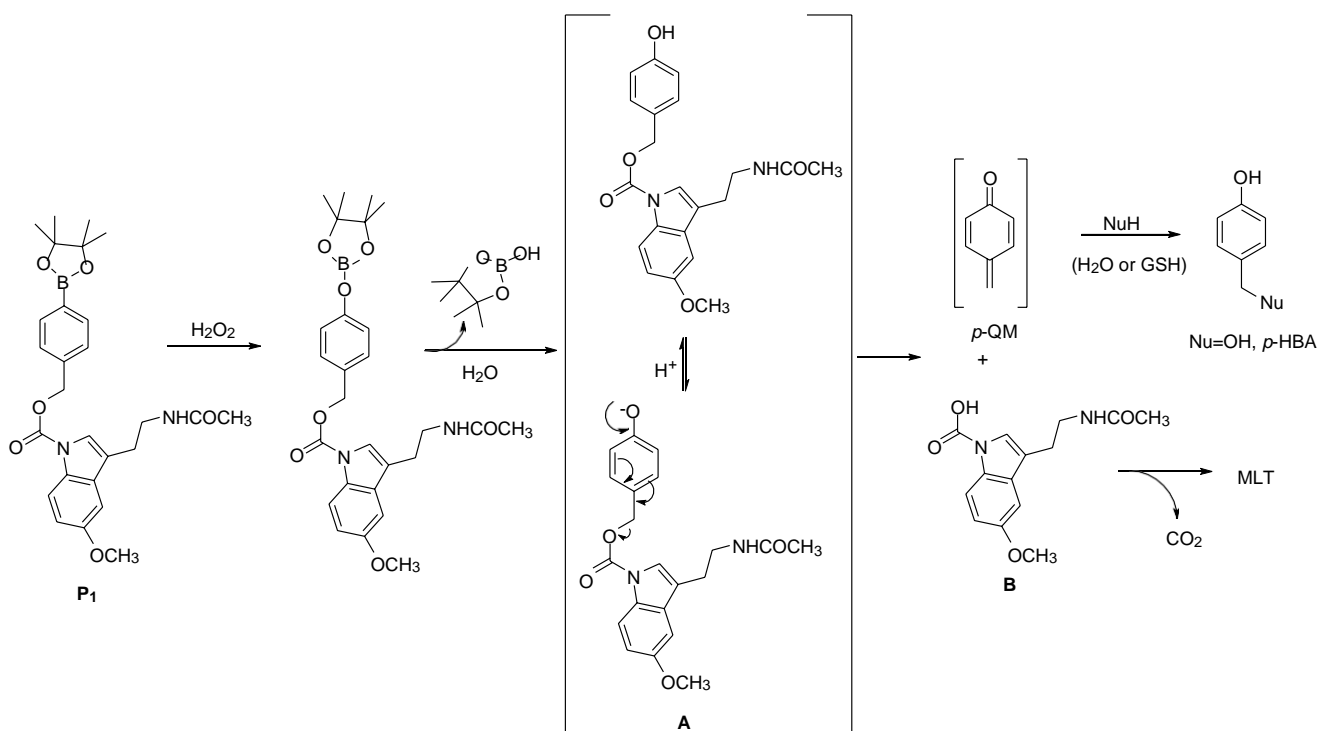


Figure 4. HPLC-DAD-MS chromatograms of the activation of **P1** by H_2O_2 (20 equiv.) in a 1:1 v/v CH_3CN/PBS .

As expected, the intensity of the **B** peak (1-carboxy-MLT) decreases with increasing incubation time, and simultaneously a consistent increase in MLT formation could be detected (Figure 4) in agreement with the putative mechanism of **P1** activation described in Scheme 2.



Scheme 2. Proposed mechanism of MLT and *p*-QM formation from **P1** and reaction of *p*-QM with different nucleophiles (e.g. H_2O or GSH).

HPLC-DAD-MS analysis showed that the H_2O_2 -induced oxidative hydroxylation of the arylboronate unit also rapidly occurred in the case of hybrid **P2**, leading to the formation of the phenol **C** ($R_t = 7.00$ min, $[\text{M}+\text{H}]^+ = 341$) (Figure 5) and of a small amount of 5-MeOT ($R_t = 2.28$ and 2.93 min) after 15 min of incubation with H_2O_2 .

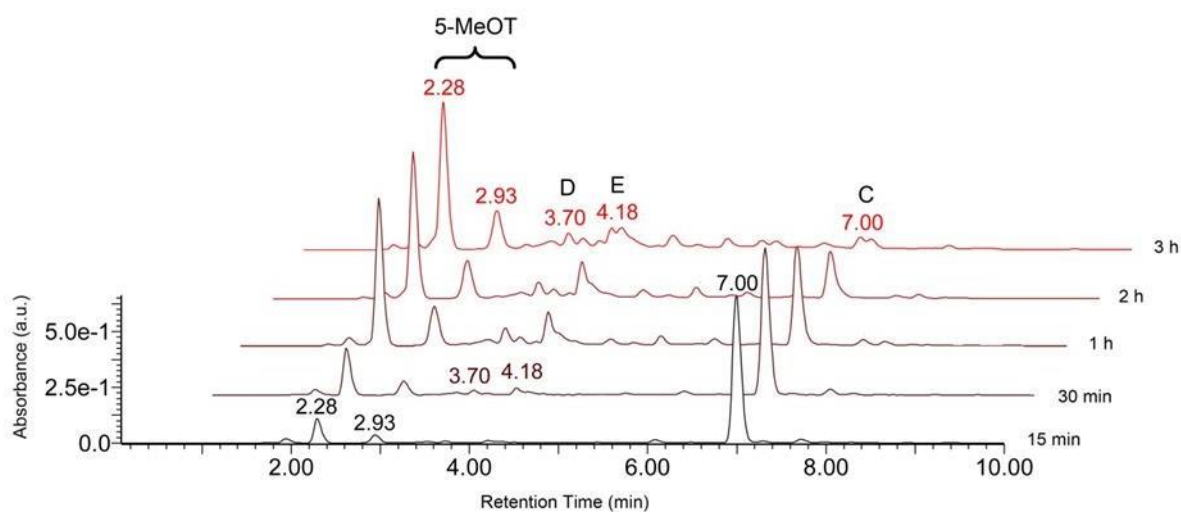


Figure 5. HPLC-DAD-MS chromatograms of the activation of **P2** by H_2O_2 (20 equiv.) in a 1:1 v/v $\text{CH}_3\text{CN}/\text{PBS}$.

The mechanism of H_2O_2 -induced activation of **P2** remains substantially the same as that of **P1**.

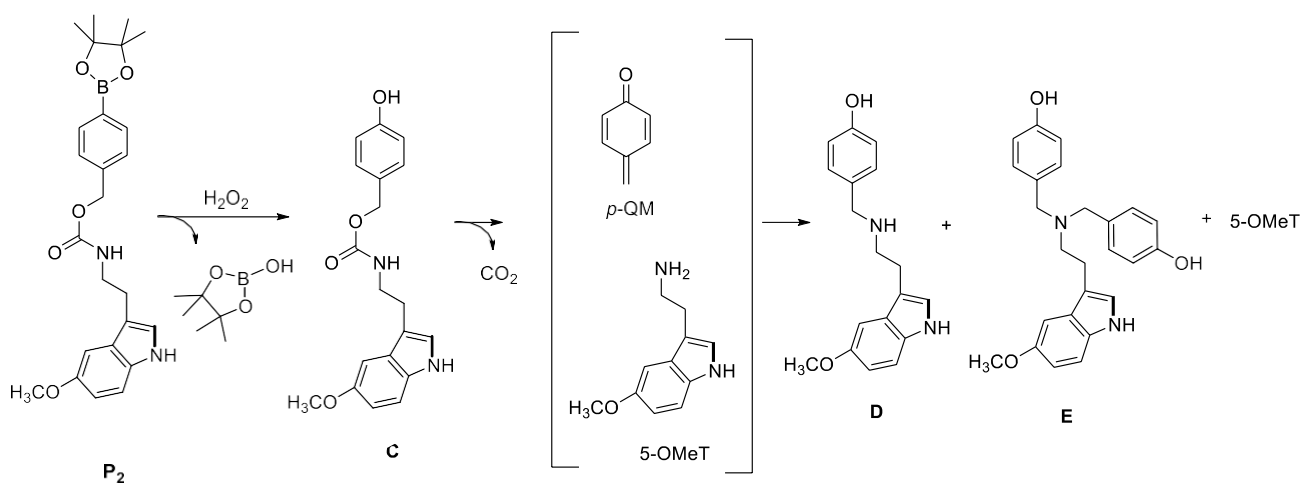
HPLC-DAD-MS analysis showed that also the arylboronate unit of hybrid **P2** was rapidly cleaved to the corresponding phenol **C** (Figure 5), after 15 min of incubation with H_2O_2 , but different from **P1**, the expected subsequent 1,6-elimination with formation of *p*-QM and 5-MeOT proceeds much more slowly.

In particular, the phenol intermediate **C** (Scheme 3) was fully decomposed only after 3 h of incubation with H_2O_2 affording 5-MeOT, little amounts of *p*-HBA and some other products, such as the adducts **D** ($R_t = 3.70$ min, $[\text{M}+\text{H}]^+ = 297$) and **E** ($R_t = 4.18$ min, $[\text{M}+\text{H}]^+ = 403$), deriving from the reaction of 5-MeOT with one or two molecules of *p*-QM (Figure 5 and Scheme 3); the formation of the latter products, probably due to the presence of the more nucleophilic 5-MeOT, indirectly confirms the release of electrophilic *p*-QM also from **P2**.

In the chromatogram illustrated in Figure 5, 5-MeOT appeared as two splitted peaks ($R_t = 2.28$ and 2.93 min), sharing the same UV profile and m/z value $[\text{M}+\text{H}]^+ = 191$; one possible cause of this peak

fragmentation is a difference in the elution strength between the diluent and the mobile phase (see Figure S3 and references⁵¹⁻⁵² for similar peak splitting).

These observations suggest that both hybrids **P1** and **P2** quickly undergo a selective oxidative hydroxylation of the arylboronate trigger unit by H₂O₂ resulting in the corresponding intermediates **A** or **C** (Schemes 2 and 3 respectively). However, subsequent release of the electrophilic *p*-QM was more rapid and consistent from hybrid **P1** (in comparison to **P2**), due to additional thermodynamic driving force from the release of the more stable leaving group 1-carboxy-MLT (compared to *N*-carboxy-tryptamine) in the cascade reaction. These results are consistent with 1,6-elimination of the leaving group being the rate determining step in this process; the relative stability of the leaving group strongly affect *p*-QM release.



Scheme 3. Proposed mechanism of H₂O₂-induced transformation of the hybrid **P2**.

Bioactivation of hybrids P1 and P2 within cells by endogenously produced H₂O₂. Having established that the indoleboronate derivatives, **P1** and **P2**, could be effectively activated *in vitro* by H₂O₂, their bioactivation in cells by endogenously produced H₂O₂ was indirectly assessed by measuring Nrf2 activation. In fact, *p*-QM rapidly reacts with –SH groups, including cysteine residues of the Nrf2 inhibitor Keap1, leading to accumulation and nuclear translocation of the transcription

factor.⁵³ To this end, NCTC-2544 cells were incubated o/n. with serum-free medium (-FBS) in the absence (NT) or presence of MLT, **P1** and **P2** (100 μ M). Then, the media were substituted with complete medium (+FBS) to induce intracellular H₂O₂ production according to Onumah et al.⁵⁴ No toxicity was detected after o/n incubation of all compounds in serum-free medium (data not shown). Western immunoblotting analysis of nuclear extracts demonstrates that Nrf2 was almost undetectable after o/n incubation in all the experimental conditions (Figure 6, panel A, lines 1-4). Upon FBS stimulation, the transcription factor was strongly activated by **P1** and to a lesser extent by **P2** (Figure 6 panel A, lines 6 and 7), in agreement with the in vitro observation of a slower release of *p*-QM from the **P2** hybrid. A modest increase in Nrf2 nuclear levels was also observed in MLT-treated and NT cells (Figure 6 panel A, lines 5 and 8), according to previous observations that MLT can suppress degradation of Nrf2 and enhance its nuclear translocation.²¹ Thus, it cannot be excluded that the higher nuclear Nrf2 accumulation induced by **P1** respect to **P2** could also result from the additive effect of the simultaneous *p*-QM and MLT release. The ability of **P1** to induce Nrf2 activation was further investigated and demonstrated to be time- and dose-dependent (Figure 6 panel B and C). Moreover, it was completely abrogated when cells were co-treated with the highly nucleophile GSH-C4, a membrane soluble GSH derivative⁴⁷ able to prevent Keap1 oxidation and Nrf2 activation by trapping ROS and reacting with *p*-QM

Altogether, these results demonstrate that the H₂O₂-induced activation of the hybrid molecules occurs within cells, consistently with the activation of Nrf2 by the released *p*-QM.

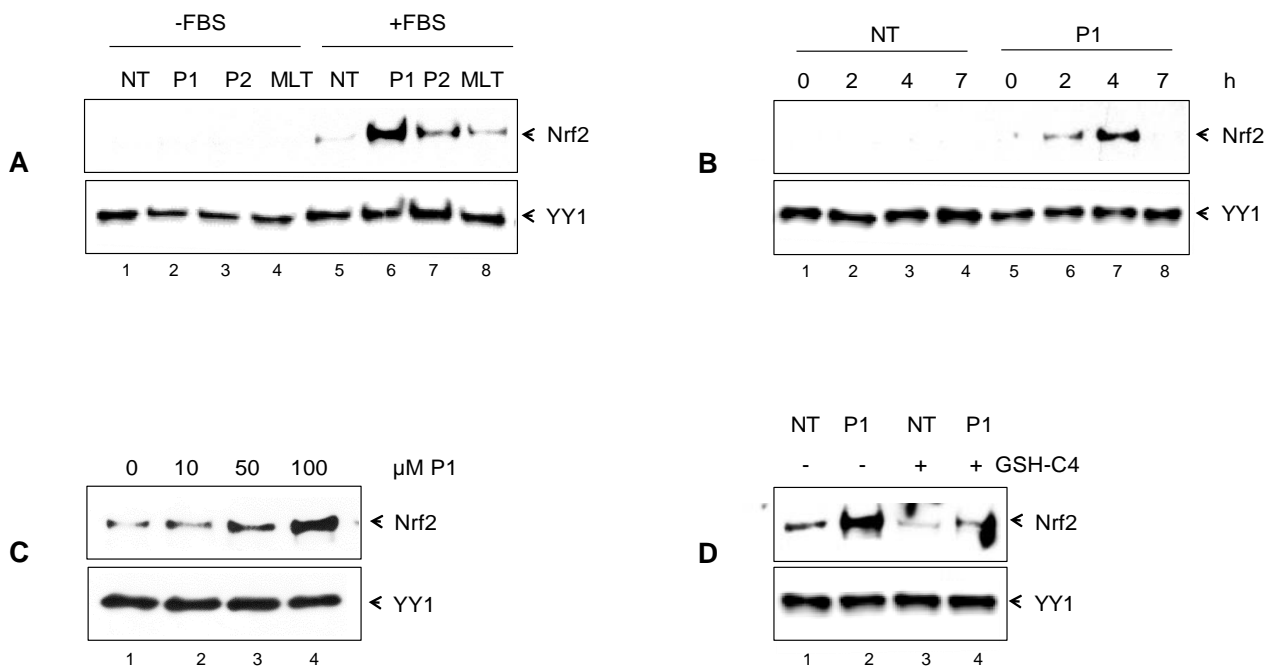


Figure 6. Western immunoblotting analysis to assess Nrf2 activation as a marker of *p*-QM release. Five μ g of nuclear extracts were loaded onto a 7% polyacrylamide gel, electroblotted and immunoblotted with an antibody against Nrf2. YY1 was stained as nuclear loading control. (A) Cells left untreated (NT) or treated with 100 μ M molecule o/n before (lines 1-4) and after 4 h of FBS-stimulation (lines 5-8). (B) Cells untreated (NT) or incubated o/n with 100 μ M **P1** in serum-free medium at different times after FBS stimulation. (C) Cells treated o/n with different concentrations of the **P1** after 4 h of FBS stimulation. (D) Cells incubated o/n with 100 μ M **P1** after 4 h of FBS stimulation in the presence of 10 mM GSH-C4. Pictures of panel A, B and C are representative of two independent experiments showing similar trends.

Potential protection by P1 against oxidative stress induced by H₂O₂. The ability of **P1** to efficiently activate Nrf2 prompted us to investigate its potential protective effects against ROS-related oxidative stress.

To simulate a condition of oxidative stress, we treated the cells with cytotoxic doses of H₂O₂ (25 and 50 μ M) for 2 h and observed a dose dependent reduction of cell viability (15 and 50%, respectively) (Figure 7, left). Pre-treatment of NCTC-2544 cells with **P1** (10, 50, 100 μ M) did not provide any

protection against H₂O₂-mediated oxidative stress. At the highest doses (50 and 100 μM), cell viability was even further reduced with respect to untreated cells at both the H₂O₂ concentrations used.

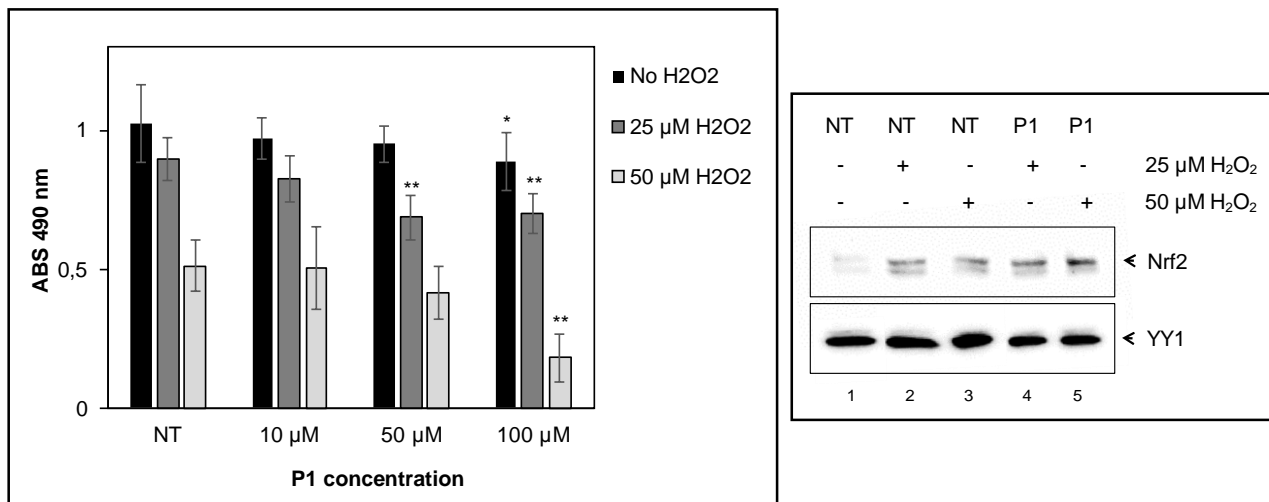


Figure 7. Cell viability and Nrf2 activation in NCTC-2544 cells pre-treated with **P1** and then exposed to H₂O₂. Left: Cells left untreated (NT) or pretreated with different concentrations of **P1** o/n, were challenged with H₂O₂ for 2 h. At the end of the incubation time, the MTS reagent was added into each well and incubated for 30 min at 37°C. The plates were read in a microplate reader at 490 nm at a reference wavelength of 630 nm. Data are the mean \pm SD of three separate experiments each carried out on eight replicates. * $p < 0.05$; ** $p < 10^{-3}$ vs NT or NT challenged with the same concentration of H₂O₂. Right: western immunoblotting analysis of Nrf2 activation. Cells were pretreated with 100 μM P1 o/n and then exposed to 25 or 50 μM H₂O₂ for 2 h as described above. Five μg of nuclear extracts were loaded onto a 7% polyacrylamide gel, electroblotted and immunoblotted with an antibody against Nrf2. YY1 was stained as nuclear loading control.

The increased cytotoxicity observed at the highest doses of the hybrid **P1** suggests that the products released after H₂O₂ treatment could exert cytotoxic effects which may predominate over the beneficial

effects expected from the Nrf2 regulated activation of the antioxidant response. Indeed, analysis of Nrf2 activation revealed that the factor was only modestly activated in cells challenged with H₂O₂ for 2 h, even in cells pretreated with 100 μM **P1** (Figure 7, right). This result is consistent with the evidence that after 2 h Nrf2 levels induced by **P1**, bioactivated by endogenously generated H₂O₂, are still very low (Figure 6, lane 6). Hence, **P1** is not effective in counteracting the cytotoxic effects of H₂O₂ since the timing of Nrf2 activation may happen later than H₂O₂- and *p*-QM-induced damage. Thus, the mounting of late defense mechanisms is inefficient in cell protection.

Cytotoxicity of hybrids P1 and P2 in NCTC-2544 and HeLa cells. Tumor cells produce high levels of ROS, which make them distinctly different from normal cells.⁵⁵ A putative strategy for selective destruction of tumor cells involves the use of cytotoxic drugs, including QM-based prodrugs, which can be activated by endogenously generated H₂O₂.^{56,57} Examples of arylboronate analogues which can be activated by H₂O₂ to form QMs and directly alkylate DNA,^{58,59} or amplify oxidative stress in cancer cells by alkylating GSH⁶⁰ have been already reported.

Thus, we preliminarily tested whether the molecules were activated in HeLa cells, a very well-known and broadly used human cancer cell line. Cells were cultured with 100 μM **P1** or **P2** for different times and then harvested to assess Nrf2 activation as marker of molecule bioactivation. Results shown in Figure 8 demonstrate that both molecules were able to stimulate Nrf2 accumulation with some differences in the kinetic of activation which occurred later in **P2**- (Figure 8, lanes 6-9) respect to **P1**-treated cells (Figure 8, lines 2-5).

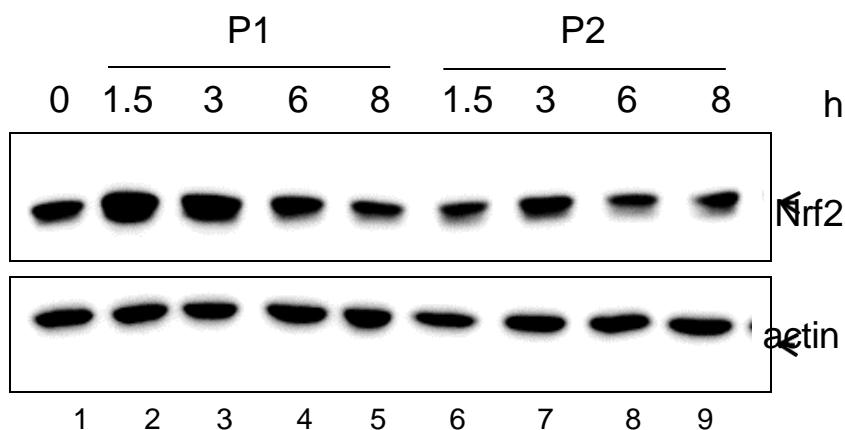


Figure 8. Western immunoblotting analysis of Nrf2 activation in HeLa cells treated with **P1** or **P2**. Cells were incubated with 100 μ M **P1** or **P2** for different times up to 8 h. Cells were lysed in SDS buffer and 40 μ g of whole cell lysates were loaded onto a 7% polyacrylamide gel, electroblotted and immunoblotted with an antibody against Nrf2. Actin was stained as loading control. Picture is representative of two independent experiments showing similar trends.

To evaluate the activity and selectivity of our hybrid compounds we measured cell viability in normal NCTC-2544 and tumoral HeLa cell lines at concentrations ranging from 0 to 100 μ M for 24 h. The highest concentration of **P1** and **P2** (100 μ M) led to approximately 26% and 12% cell death in NCTC-2544 cells, respectively, when compared to untreated cells (black and dark gray columns, Figure 8). By contrast, MLT and 5-MeOT had no toxic effects at all the tested doses (light gray columns, left and right respectively, Figure 9). No toxicity was observed in the cells grown in medium containing only the vehicle (i.e. 0.1% v/v DMSO) (data not shown).

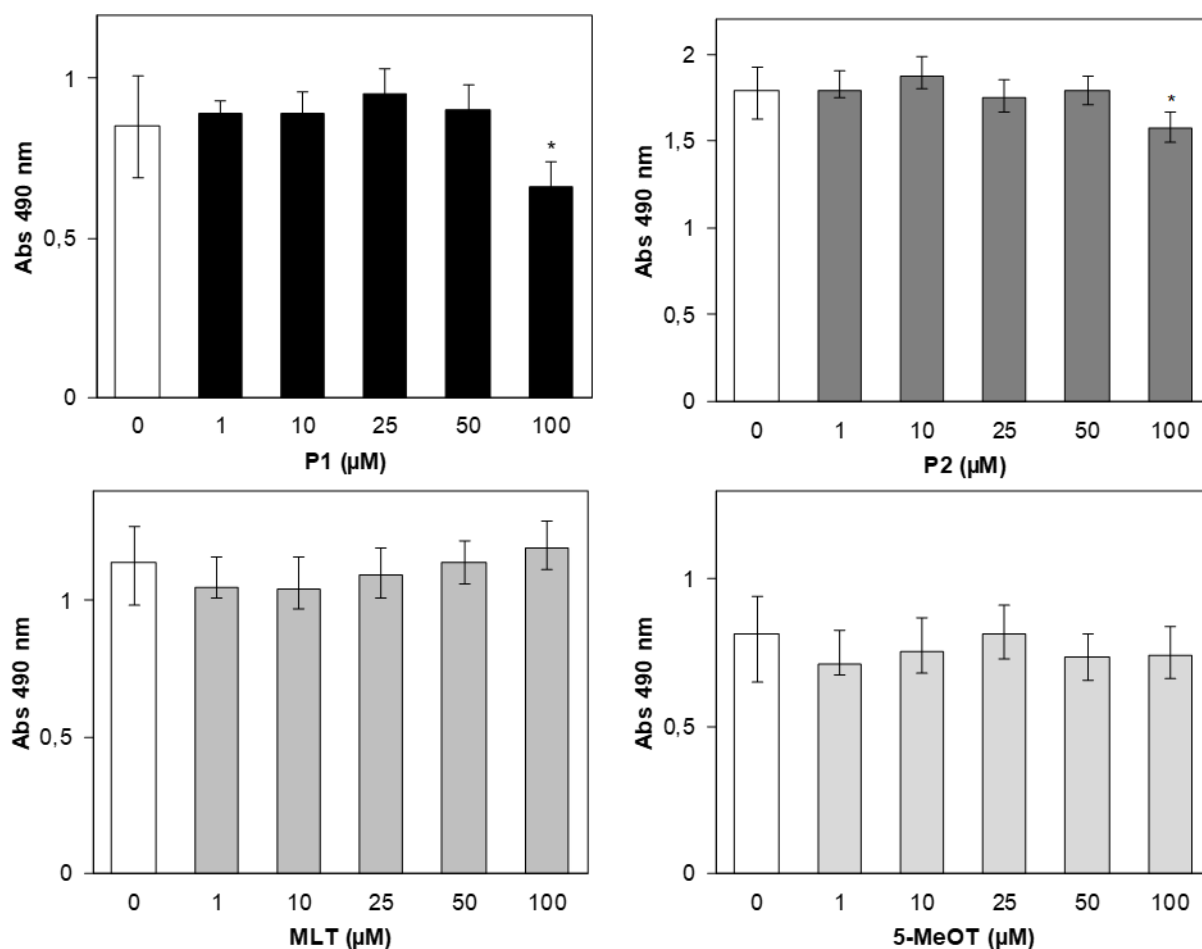


Figure 9. Cell viability in NCTC-2544 cells exposed to **P1**, **P2**, MLT and 5-MeOT. The cells were seeded in 96-well microtiter plates at a density of 5×10^3 cells/well and subsequently exposed to **P1**, **P2**, MLT and 5-MeOT at increasing concentrations (1-100 μM) for 24 h. At this time, 20 μl of MTS were added into each well, and then incubated for 30 min at 37°C . The plates were read in a microplate reader at 490 nm at a reference wavelength of 630 nm. Data are the mean \pm SD of three separate experiments each carried out in eight replicates. * $p < 0.05$ vs not treated cells (0 μM).

Based on these findings, the effects of our molecules were then studied in the tumoral HeLa cell line at the concentrations of 10, 50, 100 μM for 24 h. All the compounds showed a dose-dependent cytotoxicity when compared to untreated cells (Figure 9). Specifically, cell viability was almost

unaffected by 10 μM of all molecules, while a dose-related decrease of cell viability was observed with concentrations of 50 and 100 μM of **P1**, **P2** and MLT. In detail, hybrid **P1** was the most cytotoxic and statistically significant differences were found at 100 μM versus **P2** and MLT (Figure 10). These results are compatible with the slower bioactivation of **P2** to the *p*-QM, compared to **P1** and, to a lesser extent, to the release of MLT from **P1**. Supporting this hypothesis, cytotoxicity tests performed to determine the toxic effects of the combination of **P2** with MLT (both 100 μM) revealed an effect similar to that exerted by **P1** (data not shown). At 100 μM , the cytotoxic action of both hybrids was more evident in HeLa cells than in NCTC-2544 cells, while, at 50 μM , cell death was only observed in HeLa cells (Figures 9 and 10). These data are consistent with an overproduction of ROS in cancer cells, as demonstrated below (Figure 11), which can activate our hybrid compounds more efficiently than in normal cells. However, even if Nrf2 levels persist for long times (up to 8 h, Figure 8), they are not sufficient to defend cells from death. Normal and tumoral cells seem to respond differently also to MLT treatment, i.e. cell viability of NCTC-2544 cells is not affected by MLT while the highest concentrations of MLT are able to display cytotoxic action towards HeLa cells (Figures 9 and 10 dark gray, left). On the contrary 5-MeOT treatment did not exert significant cytotoxic effect both in NCTC-2544 and HeLa cells (Figures 9 and 10 light gray, right).

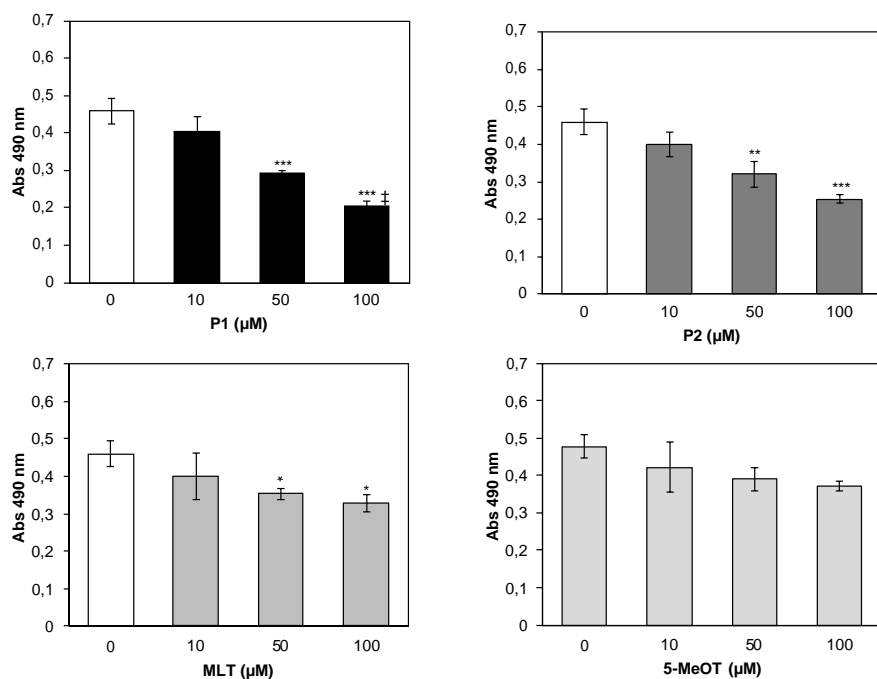


Figure 10. Cell viability in HeLa cells exposed to **P1**, **P2**, MLT and 5-MeOT. The cells were seeded in 96-well microtiter plates at a density of 2×10^3 cells/well and subsequently exposed to **P1**, **P2**, MLT and 5-MeOT at 10, 50, 100 μM for 24 h. At this time, 20 μl of MTS were added into each well, and then incubated for 30 min at 37°C . The plates were read in a microplate reader at 490 nm at a reference wavelength of 630 nm. Data are the mean \pm SD of three separate experiments each carried out in eight replicates. Data were analyzed with one-way analysis of variance (ANOVA). * $p < 0.05$ vs not treated cells (0 μM); ‡ $p < 0.05$ vs cells treated with **P2** or MLT or 5-MeOT (100 μM); ** $p < 0.01$, *** $p < 0.001$ vs not treated cells (0 μM).

To assess whether *p*-QM or MLT released from **P1** could interfere with MTS assay, some data points were confirmed by trypan blue assay. **P1**-treated HeLa cells, which provided more relevant results, were used in the elucidation of cytotoxicity effects. The results confirmed those obtained by MTS assay, in fact no toxicity was observed with 10 μM **P1** while about 25% and 40% dead cells were measured in HeLa cells treated with 50 μM and 100 μM **P1** respectively (Figure S4).

Intracellular levels of GSH and ROS in NCTC-2544 and HeLa cells. To explain the differences between the cytotoxic effects of hybrids **P1** and **P2** in HeLa compared to NCTC-2544 cells, the GSH content and ROS levels in both cell lines were investigated. HeLa cells treated with **P1** or **P2** showed consistent reduction in the level of intracellular GSH in comparison with untreated cells (Figure 11, right). Interestingly, treatment of HeLa cells with **P1** and **P2** led to dramatic decrease in GSH content (from about 82 picomoles GSH/ μ g protein in not treated cells to about 40 and 64 picomoles GSH/ μ g protein in the cells treated with **P1** and **P2** respectively), while a moderate reduction was observed in normal NCTC-2544 cells (from about 96 picomoles GSH/ μ g protein in not treated cells to about 74 and 80 picomoles GSH/ μ g protein in the cells treated with **P1** and **P2** respectively). Regarding the content of ROS, as expected, untreated HeLa cells showed higher basal intracellular ROS concentrations compared to NCTC-2544 cells (Figure 11, left). **P2** treatment did not affect ROS levels in NCTC-2544 cells and induced a moderate rightward shift of DCF fluorescence in HeLa cells. On the contrary, **P1** increased ROS level in both cell lines but only in HeLa cells the fold increase vs untreated cells (NT) was statistically significant. All these results are compatible to a preferential bioactivation of our hybrid compounds in cancer cells that overproduce ROS, generating higher levels of the GSH-scavenging *p*-QM and a consequent further increase in ROS levels above the threshold, not compatible with HeLa cells survival.

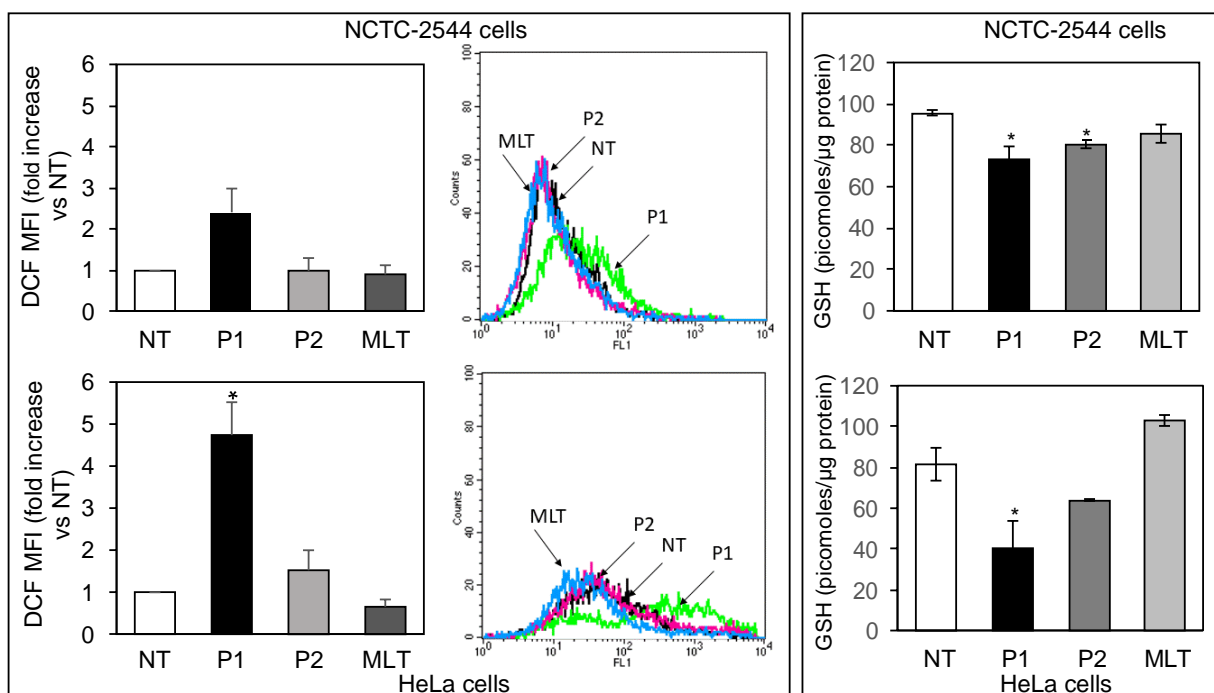


Figure 11. Left: Production of ROS in NCTC-2544 (top panels) and HeLa cells (bottom panels). Bars represent mean of fold increase of DCF fluorescence intensity (DCF MFI) in cells treated with 100 μM of **P1**, **P2** and MLT o/n compared to the untreated sample (NT). In each sample, 10,000 events were counted and each experiment was conducted in duplicate and repeated at least three times. * $p < 0.05$ vs untreated cells (NT).

Right: GSH content in NCTC-2544 cells (top panel) and HeLa cells (bottom panel) either untreated or treated with 100 μM of **P1**, **P2** and MLT o/n. Briefly, after treatments, the cells were washed and lysed with 100 μL of lysis buffer (0.1% Triton X-100, 0.1 M Na_2HPO_4 , 5 mM EDTA, pH 7.5). Thereafter, 15 μL of 0.1 N HCl and 140 μL of precipitating solution (100 ml containing 1.67 g of glacial *meta*-phosphoric acid, 0.2 g of disodium EDTA, 30 g of NaCl), were added. After centrifugation, the supernatant was collected and 25% (v/v) 0.3 M Na_2HPO_4 and immediately after 10% (v/v) DTNB were added. The mixture was stirred for 1 min at RT, then left at RT for another 5 min, and finally used for HPLC determination of GSH. Unpaired data were analyzed with the Student's t-test with Welch correction. * $p < 0.05$ vs untreated cells (NT).

Altogether, these findings are in agreement with the above cytotoxicity data showing a higher death rate in HeLa cells while leaving healthy cells relatively untouched (Figures 9 and 10).

Regarding MLT action, we can observe that it did not affect the intracellular total ROS and GSH contents in both cell lines. Thus, it seems that the cytotoxic effect exerted by MLT on HeLa cells (Figure 10) cannot be ascribed to pro-oxidant action²⁹, but presumably to pro-apoptotic effects, which have recently been described in the same cellular model.⁶¹

CONCLUSIONS

In summary, we designed and synthesized two novel arylboronate-MLT derivatives (**P1** and **P2**) that, inactive in themselves, are activated by high level of hydrogen peroxide found in cancer cells, to release *p*-QM and MLT or 5-MeOT. These compounds were initially investigated for their potential cytoprotective activity against damage from oxidative stress in normal cells, but no chemopreventive effect was observed. By contrast both studied compounds displayed cytotoxic effects against HeLa cancer cells, while normal cells were not significantly affected. Compound **P1**, which rapidly releases MLT and *p*-QM, was the most effective compound in reducing tumor HeLa cell viability. Even if MLT contributes to the observed cytotoxicity, depletion of intracellular antioxidant GSH by the released electrophilic *p*-QM, seems to be the key contributor to the biological activity. The present preliminary in vitro study contributes to the development of new “intelligent” molecules designed to be preferentially bioactivated in the presence of cancer-specific H₂O₂ concentrations.

Supporting Information

HPLC trace of an authentic sample of *p*-hydroxybenzyl alcohol (*p*-HBA) and its UV spectra, HPLC chromatogram of **P1** activation by H₂O₂ and relative identification of *p*-HBA (UV spectra), HPLC trace of an authentic sample of 5-MeOT in two different chromatographic conditions, trypan blue assay after exposure of HeLa cells to **P1**.

Author Information

Corresponding Authors:

Gilberto Spadoni

*Phone: +39 0722 303322; Fax: + 39 0722 303313; E-mail: gilberto.spadoni@uniurb.it.

Laura Chiarantini

*Phone: +39 0722 305220; E-mail: laura.chiarantini@uniurb.it.

Funding

We are grateful to University of Urbino Carlo Bo for partial financial support to this research.

Acknowledgements

The authors thank Dr. Francesca Bartoccini for support in HPLC analyses.

Notes

The authors declare no competing financial interest.

Abbreviations

5-MeOT, 5-methoxytryptamine; ARE, Antioxidant Response Element; DBU, 1,8-diazabicyclo[5.4.0]undec-7-ene; DCF, 2',7'-dichlorofluorescein, DMEM, Dulbecco's Modified Eagle Medium; DMSO, dimethyl sulfoxide; DTNB, 5,5'-dithio-bis(2-nitrobenzoic acid; EDTA, ethylenediaminetetraacetic acid; EtOAc, ethyl acetate; FBS, fetal bovine serum; GSH, glutathione; GSH-C4, N-butanoyl glutathione; H2-DCF, 2',7'-dichlorodihydrofluorescein; H2-DCF-DA, 2',7'-dichlorodihydrofluorescein diacetate; HeLa, human epithelioid cervix carcinoma cell line; MFI, mean fluorescence intensity; MLT, melatonin; MT₁, melatonin receptor subtype 1; MT₂, melatonin receptor subtype 2; MTS, (3-(4,5-dimethylthiazol-2-yl)-5-(3-carboxymethoxyphenyl)-2-(4-sulfophenyl)-2H-tetrazolium) tetrazolium assay; NCTC-2544, human keratinocyte cell line; Nrf2, nuclear factor

erythroid 2-related factor 2; *p*-HBA, *p*-hydroxybenzyl alcohol; *p*-QM, *p*-benzoquinone methide; ROS, reactive oxygen species, RT, room temperature; TEA, triethylamine; YY1, anti Ying Yan 1 antibody.

REFERENCES

- (1) Dasuri, K., Zhang, L., and Keller, J. N. (2013) Oxidative stress, neurodegeneration, and the balance of protein degradation and protein synthesis. *Free Radic. Biol. Med.* 62, 170–185.
- (2) Schumacker, P. T. (2006) Reactive oxygen species in cancer cells: Live by the sword, die by the sword. *Cancer Cell* 10, 175-176.
- (3) Li, H., Horke, S., and Forstermann, U., (2013) Oxidative stress in vascular disease and its pharmacological prevention. *Trends Pharmacol. Sci.* 34, 313–319.
- (4) Teodoro, J. S., Gomes, A. P., Varela, A. T., Duarte, F. V., Rolo, A. P., and Palmeira, C. M., (2013) Uncovering the beginning of diabetes: the cellular redox status and oxidative stress as starting players in hyperglycemic damage. *Mol. Cell. Biochem.* 376, 103–110.
- (5) Moi, P., Chan, K., Asunis, I., Cao, A., and Kan, Y. W. (1994) Isolation of NF-E2-related factor 2 (Nrf2), a NF-E2-like basic leucine zipper transcriptional activator that binds to the tandem NF-E2/AP1 repeat of the beta-globin locus control region. *Proc. Natl. Acad. Sci. U.S.A.* 91, 9926–9930.
- (6) Ma, Q. (2013) Role of nrf2 in oxidative stress and toxicity. *Annu. Rev. Pharmacol. Toxicol.* 53, 401–426.
- (7) Hayes, J. D. and Dinkova-Kostova, A. T. (2014) The Nrf2 regulatory network provides an interface between redox and intermediary metabolism. *Trends Biochem. Sci.* 39, 199–218.
- (8) Sporn, M. B., and Liby, K. T., (2012) NRF2 and cancer: the good, the bad and the importance of context. *Nat. Rev. Cancer*, 12, 564-571.
- (9) Kumar, H., Kim, I-S., More, S. V., Kim B-W., and Choi D-K. (2014) Natural product-derived pharmacological modulators of Nrf2/ARE pathway for chronic diseases. *Nat. Prod. Rep.*, 31, 109–139.
- (10) Tong, L., Chuang, C. C., Wu, S., and Zuo, L. (2015) Reactive oxygen species in redox cancer therapy. *Cancer Lett.* 367, 18-25.
- (11) Yang, Y., Karakhanova, S., Werner, J., and Bazhin, A. V. (2013) Reactive oxygen species in cancer biology and anticancer therapy. *Curr. Med. Chem.* 20, 3677-3692.
- (12) Trachootham, D., Alexandre, J., and Huang, P. (2009) Targeting cancer cells by ROS-mediated mechanisms: a radical therapeutic approach? *Nat. Rev. Drug Discov.* 8, 579-591.
- (13) Raj, L., Ide, T., Gurkar, A. U., Foley, M., Schenone, M., Li, X., Tolliday, N. J., Golub, T. R., Carr, S. A., Shamji, A. F., Stern, A. M., Mandinova, A., Schreiber, S. L., and Lee, S. W. (2011) Selective killing of cancer cells with a small molecule targeting stress response to ROS. *Nature* 475, 231–234.

- (14) Liu, J., Clough, S. J., Hutchinson, A. J., Adamah-Biassi, E. B., Popovska-Gorevski, M., Dubocovich, M. L. (2016) MT₁ and MT₂ melatonin receptors: a therapeutic perspective. *Annu. Rev. Pharmacol. Toxicol.* 56, 361–383.
- (15) Hardeland, R., Cardinali, D. P., Srinivasan, V., Spence, D. W., Brown, G. M., Pandi-Perumal, S.R. (2011) Melatonin-a pleiotropic, orchestrating regulator molecule. *Prog. Neurobiol.* 93, 350–384.
- (16) Gatti, G., Lucini, V., Dugnani, S., Calastretti, A., Spadoni, G., Bedini, A., Rivara, S., Mor, M., Canti, G., Scaglione, F., and Bevilacqua, A. (2017) Antiproliferative and pro-apoptotic activity of melatonin analogues on melanoma and breast cancer cells. *Oncotarget* 8, 68338-68353.
- (17) Alghamdi, B. S. (2018) The neuroprotective role of melatonin in neurological disorders. *J. Neurosci. Res.* 96, 1136-1149
- (18) Jockers, R., Delagrang, P., Dubocovich, M. L., Markus R. P., Renault N., Tosini, G., Cecon E., and Zlotos, D. P. (2016) Update on melatonin receptors: IUPHAR Review 20. *Br. J. Pharmacol.* 173, 2702–2725.
- (19) Reiter, R. J. Mayo, J. C., Tan, D. X., Sainz, R. M., Alatorre-Jimenez, M., and Qin, L. (2016) Melatonin as an antioxidant: under promises but over delivers. *J Pineal Res.* 61, 253-78.
- (20) Wang, Z., Ma, C., Meng, C. J., Zhu, G. Q., Sun, X. B., Huo, L., Zhang, J., Liu, H. X., He, W. C., Shen, X. M., Shu, Z., and Chen, G. (2012) Melatonin activates the Nrf2-ARE pathway when it protects against early brain injury in a subarachnoid hemorrhage model. *J. Pineal Res.* 53, 129–137.
- (21) Vriend, J., and Reiter, R. J. (2015) The Keap1-Nrf2-antioxidant response element pathway: a review of its regulation by melatonin and the proteasome, *Mol. Cell. Endocrinol.* 401, 213–220.
- (22) Janjetovic, Z., Jarrett, S. G., Lee, E. F., Duprey, C., Reiter, R. J., and Slominski, A. T. (2017) Melatonin and its metabolites protect human melanocytes against UVB-induced damage: Involvement of NRF2-mediated pathways. *Sci. Rep.* 7, 1274.
- (23) Li, Y., Li, S., Zhou, Y., Meng, X., Zhang, J. J., Xu, D. P., and Li, H. B. (2017) Melatonin for the prevention and treatment of cancer. *Oncotarget.* 8, 39896–39921.
- (24) Reiter, R. J, Rosales-Corral, S. A., Tan, D. X., Acuna-Castroviejo, D. A., Qin, L., Yang, S. F., and Xu, K. (2017) Melatonin a full service anti-cancer agent: inhibition of initiation, progression and metastasis. *Int. J. Mol. Sci.* 18, 843.
- (25) Jardim-Perassi, B. V., Arbab, A. S., Ferreira, L. C., Borin, T. F., Varma, N., Iskander, A., Shankar, A., Ali, M. M., Zuccari, D. (2014) Effect of melatonin on tumor growth and angiogenesis in xenograft model of breast cancer. *PLoS One* 9, e853111.

- (26) Favero, G., Moretti, E., Bonomini, F., Reiter, R. J., Rodella, L. F., Rezzani, R. (2018) Promising antineoplastic actions of melatonin. *Front. Pharmacol.* 9, 1086.
- (27) Sanchez-Barcelo, E. J., Mediavilla, M. D., Alonso-Gonzalez, C., and Reiter, R. J. (2012) Melatonin uses in oncology: Breast cancer prevention and reduction of the side effects of chemotherapy and radiation. *Expert Opin. Inv. Drug.* 21, 819–831.
- (28) Kosar, P. A., Naziroglu, M., Ovey, I. S., and Cig, B. (2016) Synergic effects of doxorubicin and melatonin on apoptosis and mitochondrial oxidative stress in MCF-7 breast cancer cells: Involvement of TRPV1 channels. *J. Membrane Biol.* 249,129–140.
- (29) Zhang, H. M., and Zhang, Y. (2014) Melatonin: a well-documented antioxidant with conditional pro-oxidant actions. *J. Pineal Res.* 57, 131–146.
- (30) Bejarano, I., Espino, J., Barriga, C., Reiter, R. J., Pariente, J. A, and Rodríguez, A. B. (2011) Pro-oxidant effect of melatonin in human leucocytes: relation with its cytotoxic and proapoptotic effects. *Basic Clin. Pharmacol. Toxicol.* 108, 14–20.
- (31) Bizzarri, M., Proietti, S., Cucina, A., and Reiter, R. J. (2013) Molecular mechanisms of the proapoptotic actions of melatonin in cancer: a review. *Expert Opin. Ther. Targets* 17, 1483-1496.
- (32) Singh, J., Petter, R. C., Baillie, T. A., and Whitty, A. (2011) The resurgence of covalent drugs. *Nat. Rev. Drug Discovery* 10, 307–317.
- (33) Dufrasne, F., Gelbcke, M., Nève, J., Kiss, R., and Kraus, J-L. (2011) Quinone methides and their prodrugs: a subtle equilibrium between cancer promotion, prevention and cure. *Curr. Med. Chem.* 18, 3995–4011.
- (34) Dunlap, T., Chandrasena, R. E., Wang, Z., Sinha, V., and Thatcher, G. R. J. (2007) Quinone formation as a chemoprevention strategy for hybrid drugs: balancing cytotoxicity and cytoprotection. *Chem. Res. Toxicol.* 20, 1903–1912.
- (35) Hulsman, N., Medema, J. P., Bos, C., Jongejan, A., Leurs, R., Smit, M. J., de Esch, I. J., Richel, D., and Wijtmans, M. (2007) Chemical insights in the concept of hybrid drugs: the antitumor effect of nitric oxide-donating aspirin involves a quinone methide but not nitric oxide nor aspirin *J. Med. Chem.* 50, 2424–2431.
- (36) Kastrati, I., Litosh, V. A., Zhao, S., Alvarez, M., Thatcher, G. R., and Frasor, J. (2015) A novel aspirin prodrug inhibits NFκB activity and breast cancer stem cell properties. *BMC Cancer* 15, 845.
- (37) Dunlap, T., Piyankarage, S. C., Wijewickrama, G. T., Abdul-Hay, S., Vanni, M., Litosh, V., Luo, J., and Thatcher, G. R. (2012) Quinone-induced activation of Keap1/Nrf2 signaling by aspirin prodrugs masquerading as nitric oxide. *Chem. Res. Toxicol.* 25, 2725–2736.

- (38) Bolton, J. L. (2014) Quinone methide bioactivation pathway: contribution to toxicity and/or cytoprotection? *Curr. Org. Chem.* 18, 61–69.
- (39) Bolton, J. L., and Dunlap, T. (2017) Formation and Biological Targets of Quinones: Cytotoxic versus Cytoprotective Effects. *Chem. Res. Toxicol.* 30, 13–37.
- (40) Lippert, A. R., Van de Bittner, G. C., and Chang, G. J. (2011) Boronate oxidation as a bioorthogonal reaction approach for studying the chemistry of hydrogen peroxide in living systems. *Acc. Chem. Res.* 44, 793–804.
- (41) Broaders, K. E., Grandhe, S., and Frechet, J. M. J. (2011) A biocompatible oxidation-triggered carrier polymer with potential in therapeutics. *J. Am. Chem. Soc.*, 133, 756–758.
- (42) Li, J., Li, Y., He, Q., Li, Y., Li, H., and Liu, L. (2014) One-pot native ligation of peptide hydrazides enables total synthesis of modified histones. *Org. Biomol. Chem.* 12, 5435–5441.
- (43) Bartolucci, S., Mari, M., Bedini, A., Piersanti, G., and Spadoni, G. (2015) Iridium-catalyzed direct synthesis of tryptamine derivatives from indoles: exploiting N-protected β -amino alcohols as alkylating agents. *J. Org. Chem.* 80, 3217–3222.
- (44) Montenegro, L., Trapani, A., Fini, P., Mandracchia, D., Latrofa, A., Cioffi, N., Chiarantini, L., Picceri, G. G., Brundu, S., and Puglisi, G. (2014) Chitosan nanoparticles for topical co-administration of the antioxidants glutathione and idebenone: characterization and in vitro release. *Br. J. Pharmaceutical Res.* 4, 2387–2406.
- (45) Crinelli, R., Bianchi, M., Radici, L., Carloni, E., Giacomini, E., and Magnani, M. (2015) Molecular dissection of the human ubiquitin C promoter reveals heat shock element architectures with activating and repressive functions. *PLoS One* 10(8):e0136882.
- (46) Eruslanov, E., and Kusmartsev, S. (2010) Identification of ROS using oxidized DCFDA and flow-cytometry. *Methods Mol. Biol.* 594, 57–72.
- (47) Fraternali, A., Crinelli, R., Casabianca, A., Paoletti, M. F., Orlandi, C., Carloni, E., Smietana, M., Palamara, A. T., and Magnani M. (2013) Molecules altering the intracellular thiol content modulate NF- κ B and STAT-1/IRF-1 signalling pathways and IL-12 p40 and IL-27 p28 production in murine macrophages. *PLoS One* 8(3):e57866.
- (48) Brundu, S., Nencioni, L., Celestino, I., Coluccio, P., Palamara, A. T., Magnani, M., and Fraternali, A. (2016) Validation of a Reversed-Phase High Performance Liquid Chromatography Method for the Simultaneous Analysis of Cysteine and Reduced Glutathione in Mouse Organs. *Oxid. Med. Cell. Longev.* 2016:1746985.
- (49) Zielonka, J., Sikora, A., Hardy, M., Joseph, J., Dranka, B. P., Kalyanaraman, B. (2012) Boronate probes as diagnostic tools for real time monitoring of peroxynitrite and hydroperoxides. *Chem. Res. Toxicol.* 25, 1793-1799.

- (50) Hagen, H., Merzenell, P., Jentzsch, E., Wenz, F., Veldwijk, M R. and Mokhir, A. (2012) Aminoferrocene-Based Prodrugs Activated by Reactive Oxygen Species. *J. Med Chem.* 55, 924-934.
- (51) Wollinger, W., da Silva, R.A., da Nóbrega, A.B., Lopes, R.S.C., Lopes, C.C., and Slana, G.B.C.A. (2016). Assessing drug-exciptent interactions in the formulations of isoniazid tablets. *J. Braz. Chem. Soc.* 27, 826–833.
- (52) Fang, L., Yao, X., Wang, L., and Li, J. (2015). Solid-phase extraction-based ultra-sensitive detection of four lipophilic marine biotoxins in bivalves by high-performance liquid chromatography-tandem mass spectrometry. *J. Chromatogr. Sci.* 53, 373–379.
- (53) Dinkova-Kostova, A. T., Fahey, J. W., Kostov, R. V., and Kensler, T. W. (2017) KEAP1 and Done? Targeting the NRF2 Pathway with Sulforaphane. *Trends Food Sci. Technol.* 69(Pt B), 257–269.
- (54) Onumah OE, Jules GE, Zhao Y, Zhou L, Yang H, Guo Z (2009). Overexpression of catalase delays G0/G1- to S-phase transition during cell cycle progression in mouse aortic endothelial cells. *Free Radic. Biol. Med.* 46, 1658-1667.
- (55) Hileman, E. O., Liu, J., Albitar, M., Keating, M. J., and Huang, P. (2004) Intrinsic oxidative stress in cancer cells: a biochemical basis for therapeutic selectivity. *Cancer Chemother. Pharmacol.* 53, 209–219.
- (56) Peng, X., and Gandhi, V. (2012) ROS-activated anticancer prodrugs: a new strategy for tumor-specific damage. *Ther. Deliv.* 3, 823–833.
- (57) Trachootham, D., Alexandre, J., and Huang, P. (2009) Targeting cancer cells by ROS-mediated mechanisms: a radical therapeutic approach? *Nat. Rev. Drug Discov.* 8, 579–591.
- (58) Cao, S., Wang, Y., and Peng, X. (2014) The leaving group strongly affects H(2)O(2)-induced DNA cross-linking by arylboronates. *J. Org. Chem.* 79, 501–508.
- (59) Freccero, M. (2004) Quinone Methides as Alkylating and Cross-linking Agents. *Mini-reviews in Organic Chemistry 1*, 403–415.
- (60) Noh, J., Kwon, B., Han, E., Park, M., Yang, W., Cho, W., Yoo, W., Khang, G., and Lee, D. (2015) Amplification of oxidative stress by a dual stimuli-responsive hybrid drug enhances cancer cell death. *Nat. Commun.* 6, 6907.
- (61) Chen, L., Liu, L., Li, Y., and Gao, J. (2018) Melatonin increases human cervical cancer HeLa cells apoptosis induced by cisplatin via inhibition of JNK/Parkin/mitophagy axis. *In Vitro Cell. Dev. Biol. Animal.* 54, 1–10.